



Effects of Inundation by the 14th November, 2016 Kaikōura Tsunami on Banks Peninsula, Canterbury, New Zealand

EMILY M. LANE,¹ JOSE BORRERO,^{2,3} COLIN N. WHITTAKER,⁴ JO BIND,¹ CATHERINE CHAGUÉ-GOFF,⁵ JAMES GOFF,⁵ DEREK GORING,⁶ JO HOYLE,¹ CHRISTOF MUELLER,⁷ WILLIAM L. POWER,⁷ CATHERINE M. REID,⁸ JAMES H. WILLIAMS,⁸ and SHAUN P. WILLIAMS¹

Abstract—At 12:02:56 a.m. Monday, November 14 2016 NZDT (11:02:56 a.m., November 13 2016 UTC) a magnitude 7.8 earthquake struck near Kaikōura on the north-eastern coast of the South Island of New Zealand. This earthquake caused a tsunami along New Zealand's east coast that was recorded on a number of sea level gauges. Outside of the Kaikōura region, north facing bays along Banks Peninsula were most affected by the tsunami. Of these, Little Pigeon Bay experienced extensive inundation and an unoccupied cottage was destroyed by the wave run-up. We report on the inundation extent and (inferred) flow directions at Little Pigeon Bay, including a study on temporal changes in the field evidence of this inundation. Preliminary modelling results indicate that the waves may have excited resonance in the bay. We also present results from inundation surveys of nearby, north-facing bays on Banks Peninsula. The excitation of resonance in Little Pigeon Bay provides an explanation for the more severe inundation and damage there in comparison to these nearby bays.

Key words: Tsunami, inundation, Kaikōura Earthquake, Kaikōura tsunami, Kaikōura, Kaikoura, New Zealand, Little Pigeon Bay, 14 November 2016 Earthquake, Banks Peninsula.

1. Introduction

At 12:02:56 a.m. Monday, November 14 2016 NZDT (11:02:56 a.m., November 13 2016 UTC) a magnitude 7.8 earthquake struck at latitude 42.69°S, 173.02°E. The earliest estimate of the moment magnitude was given as M_w 6.5 via GeoNet (GeoNet 2016a; Kaiser et al. 2017), but this was upgraded multiple times over subsequent hours. The earthquake epicentre was located inland, thus suggesting it was unlikely to generate a tsunami. However, the proximity of the quake to Kaikōura Canyon, a potential submarine landslide source (Walters et al. 2006), meant that scientists were closely monitoring the situation. Indeed, a rapid drawdown of 2.5 m at the Kaikōura tsunami gauge alerted scientists and emergency managers that a tsunami had occurred, although it was subsequently discovered to have been generated from a fault rupture source and not a submarine failure. Figure 1 shows the location of the earthquake epicentre on the northeast coast of the South Island of New Zealand; in addition to the locations of sea level gauge measurements and field investigations discussed in this paper.

The USGS finite fault solution (USGS 2016) shows that while the earthquake was initiated inland, the bulk of the energy release occurred some 175 km NE of the epicentre. The moment rate function displays several distinct peaks of energy release, with the largest one occurring about a minute into the event and focussed off-shore of the Clarence River. Subsequent investigation has revealed a complicated rupture pattern with on- and off-shore ruptures of multiple known faults from North Canterbury and Marlborough (Kaiser et al. 2017).

While post-tsunami ground surveys of the Kaikōura coastline were planned, field investigation were delayed since the region was in a State of Emergency

¹ National Institute of Water and Atmospheric Research Limited, 10 Kyle Street, Christchurch, New Zealand. E-mail: Emily.Lane@niwa.co.nz

² eCoast Marine Consulting and Research, PO Box 151, Raglan, Waikato, New Zealand.

³ Department of Civil and Environmental Engineering, University of Southern California, Los Angeles, CA 90089-2531, USA.

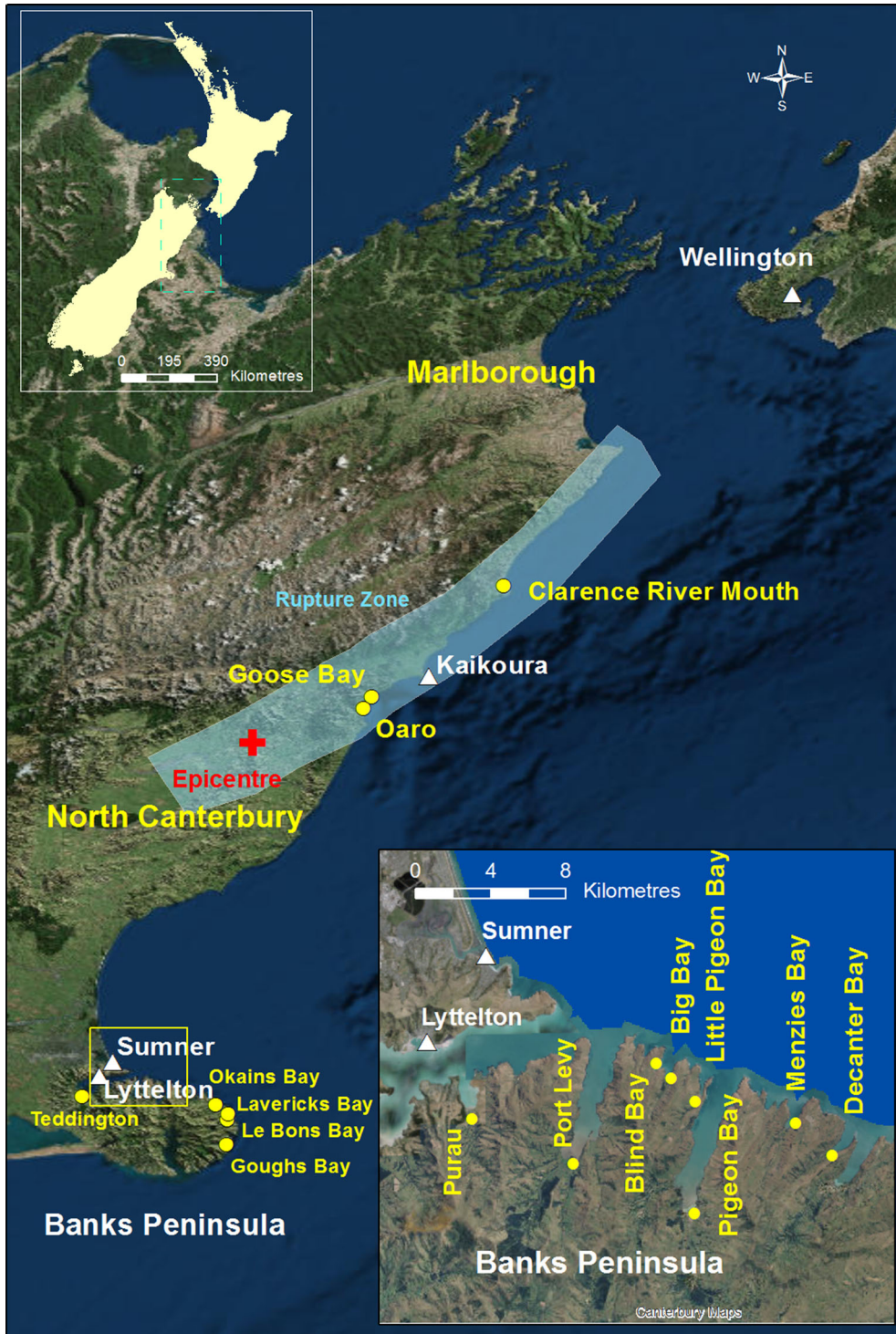
⁴ Department of Civil and Environmental Engineering, The University of Auckland, PB 92019, Auckland 1142, New Zealand.

⁵ PANGEA Research Centre, School of Biological, Earth and Environmental Sciences, UNSW Australia, Sydney, NSW 2052, Australia.

⁶ Mulgor Consulting Limited, P O Box 9320, Tower Junction, Christchurch 8149, New Zealand.

⁷ GNS Science, 1 Fairway Drive, Avalon, Wellington, New Zealand.

⁸ Department of Geological Sciences, University of Canterbury, PB 4800, Christchurch 8140, New Zealand.



and Civil Defence Emergency Management (CDEM) was focussed on the immediate aftermath. Furthermore, numerous co-seismic and post-seismic

landslides had blocked the main highway (State Highway 1) limiting access to Kaikōura Township by helicopter only. Early reconnaissance flights along the

◀Figure 1

Map showing sea level gauges (*white triangles*) and locations cited in the text (*yellow circles*), earthquake epicentre (*red cross*) and rupture zone (*shaded area*). Kaikōura Canyon lies beneath the 'O' of Oaro. *Hashed blue box on top inset* shows location of main figure, *yellow box on main figure* shows location of *bottom inset*. The main figure extends between 44.38°S and 40.42°S and between 172.45°E and 175.11°E

coast did not reveal notable evidence of tsunami inundation, although considerable coastal uplift was evident. Likewise, there were no initial reports from coastal communities of tsunami inundation. However, later ground surveys revealed evidence of inundation of several beaches and river valleys in Oaro and Goose Bay (Power et al. 2017 submitted, this issue).

On Monday afternoon (14 November 2016) a report was received through the Christchurch Press newspaper of an historic cottage in Little Pigeon Bay, Banks Peninsula that had been severely damaged by the tsunami. Since this was the only confirmed report of tsunami inundation, research efforts were focussed in that area. With an impending heavy rainstorm anticipated for Thursday 17 November, our group visited the site Wednesday 16 November to undertake an initial survey. A second field trip took place on Saturday 19 November, with further visits on Wednesday 30 November (16 days after the tsunami), and Sunday 15 January 2017 (62 days after the tsunami).

This paper presents information from tsunami gauges near Banks Peninsula (including wave heights and periods), field observations documenting evidence of inundation and temporal changes, tsunami flow patterns and damage at Little Pigeon Bay, and preliminary modelling of the bay. Reports from adjacent north-facing bays on Banks Peninsula are also presented, with a brief comparison of the impact of tsunami inundation with that observed elsewhere on the Kaikōura coast.

2. Tsunami Gauges

The Kaikōura tsunami was recorded on several tide gauges located along the east coast of New Zealand and in the Chatham Islands (see Power et al. 2017 submitted, this issue).¹ Of these, three gauges

¹ While the Kaikōura gauge was co-seismically uplifted about a metre by the tsunami, none of the other sea level gauges were moved (Power et al., submitted, this issue).

were located near Christchurch—two at Sumner Head just outside of Lyttelton Harbour and a third at the Port of Lyttelton inside Lyttelton Harbour (Fig. 1). The two Sumner gauges are operated independently, one by NIWA (NIWA 2016) and the other jointly owned by Land Information New Zealand (LINZ 2016) and New Zealand's GeoNet program (GeoNet 2016b).

Inspection of the raw data from the Sumner gauge (Fig. 2) shows the first signs of the tsunami around 1 h 15 min after the earthquake (around 1:15 a.m.) approximately midway through the rising tide. Prior to the tsunami, the water level at the Sumner gauge was close to the predicted tide level, with no measurable storm surge effect. The raw tide gauge data show a prolonged first surge lasting around 30 min before more rhythmic water surface fluctuations appear ultimately culminating in the largest oscillations between 3:00 a.m. and 5:00 a.m. (3–5 h after the earthquake). The highest absolute water level reached during the tsunami was +1.85 m relative to the Lyttelton Vertical Datum 1937 (LVD37) at 3:59 a.m. (+1.44 m above New Zealand Vertical Datum 2016 (NZVD2016)), approximately 30 min before high tide. Over the next several hours, regular oscillations continued as the amplitude gradually diminished.

To obtain a clearer picture of the tsunami signal, the raw tide gauge record was filtered to remove the effect of tide and other factors (i.e., wind and pressure effects) that cause fluctuations in the water surface. Data from the three tide gauges were processed identically using methods described in Goring and Henry (2007) and Goring (2008) and presented in Fig. 3. In this filtered record, the prolonged first surge seen on the raw Sumner record is not as prominent. The delay in arrival of the first surge between the Sumner gauges and the Lyttelton one is evident and occurs as a result of the additional travel time necessary for the tsunami to propagate up Lyttelton Harbour. From the Sumner records it is apparent that the two instruments recorded nearly identical water level data with the NIWA gauge recording slightly larger peaks and troughs. The maximum wave amplitude (Zero to Peak) at Lyttelton was +0.49 m around 3:45 a.m., while at Sumner it was +0.63 m at 3:59 a.m.

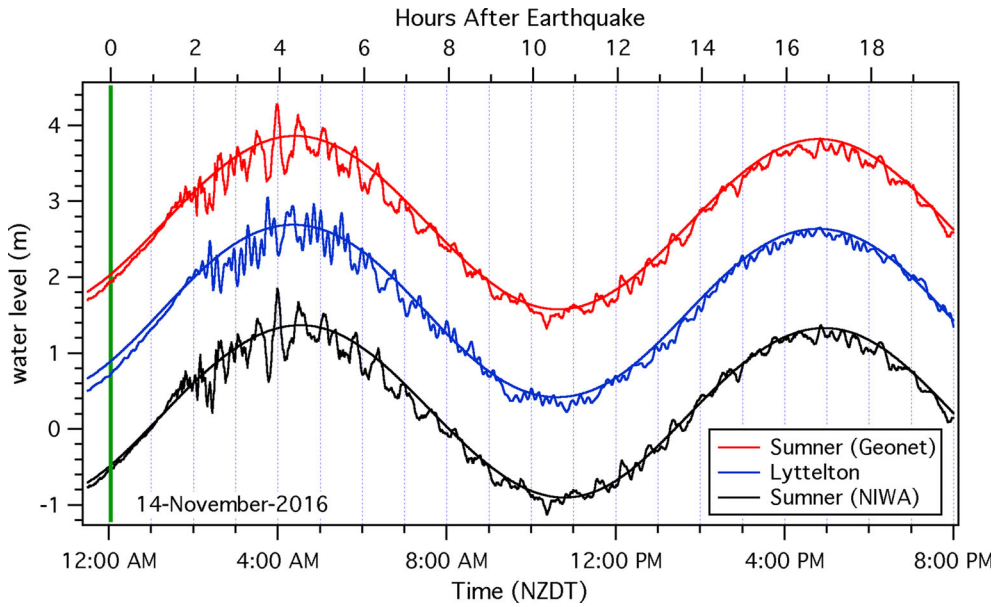


Figure 2

Predicted tide (*smooth curve*) and recorded raw water levels on the three Christchurch area tide gauges showing the effects of the Kaikōura tsunami. The NIWA Sumner gauge zero is LVD37 (0.41 m below NZVD2016), the Lyttelton and GeoNet Sumner gauges have been offset for plotting. *Vertical green line* is the earthquake origin time

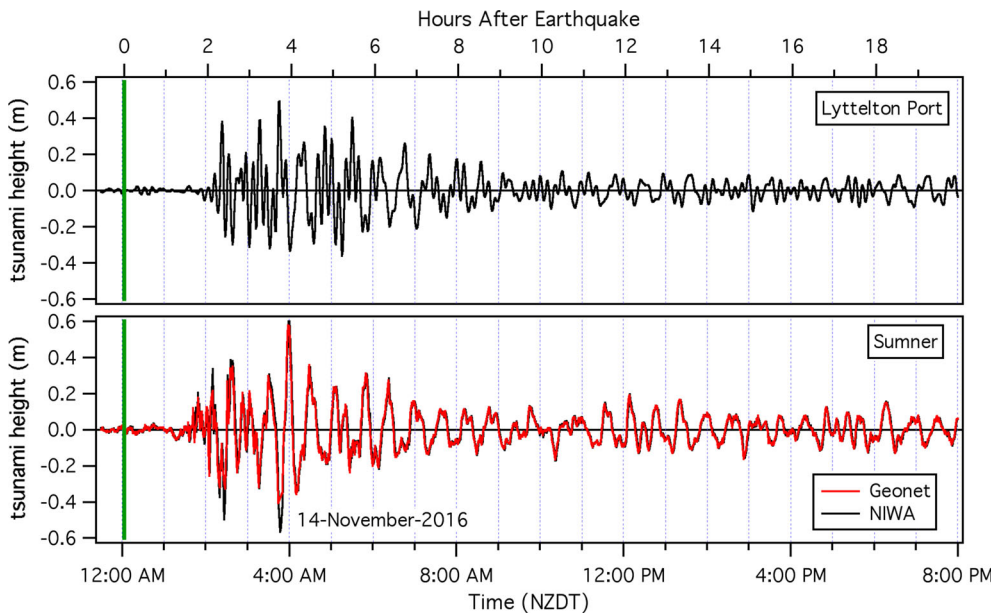


Figure 3

Filtered tide gauge records for Lyttelton Port (*top*) and Sumner (*bottom*) gauges

A zero-crossing analysis (waves are split at the zero up-crossings and the results reported at the midpoint between crossings; see also Holthuijsen

2007) on the filtered long-wave record was then used to determine the height and period of individual wave oscillations (Figs. 4, 5). On both the

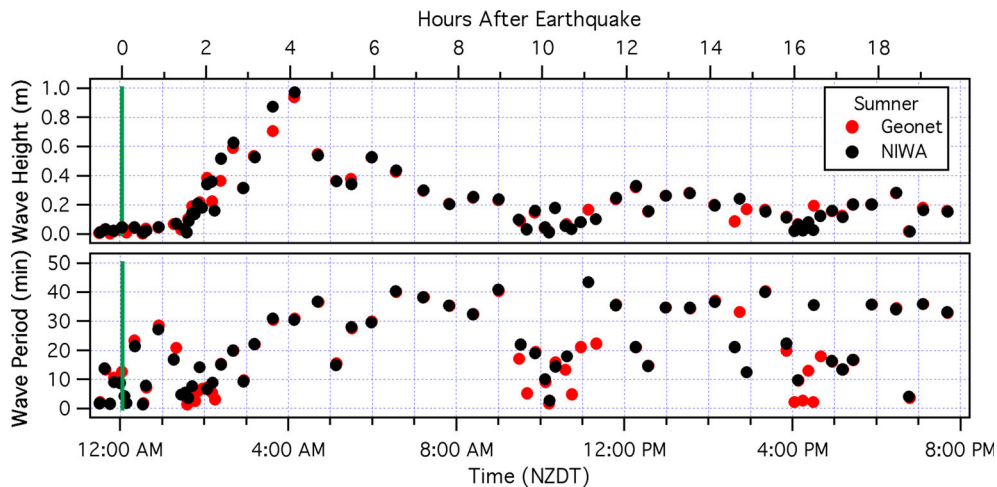


Figure 4

Wave height (peak-to-trough) (*top*) and wave period (*bottom*) of individual tsunami wave cycles from the two Sumner gauges. Vertical green line is the earthquake origin time

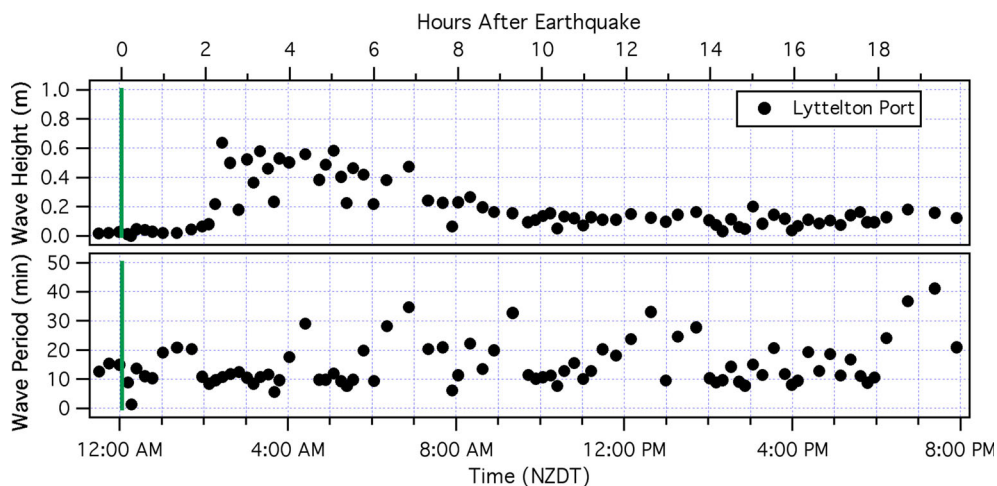


Figure 5

Wave height (peak-to-trough) (*top*) and wave period (*bottom*) of individual tsunami wave cycles from the Lyttelton Port gauge. Vertical green line is the earthquake origin time

Sumner and Lyttelton gauges there was some long wave energy present prior to the tsunami arrival—apparent from the presence of waves with 10–30 min periods seen on all three records. However, the heights of these wave cycles were small, on the order of <math>< 5\text{ cm}</math>. As the tsunami arrived (at approximately 1:15 a.m. at Sumner and 1:30–2:00 a.m. at Lyttelton Port), the wave heights steadily increased along with the wave periods peaking at approximately 4:00 a.m. NZDT.

It is interesting to note that the largest individual measured wave height (peak-to-trough) from the Kaikōura tsunami (other than on the Kaikōura tide gauge located in the immediate source region: Power et al. 2017 submitted, this issue) occurred at Sumner, and was recorded as 0.93 m (Geonet) and 0.98 m (NIWA). This wave had a period of 30 min and occurred at about 4:00 a.m. (~ 4 h after the earthquake). Waves in Lyttelton Harbour were smaller, but there were multiple waves with heights around 0.6 m

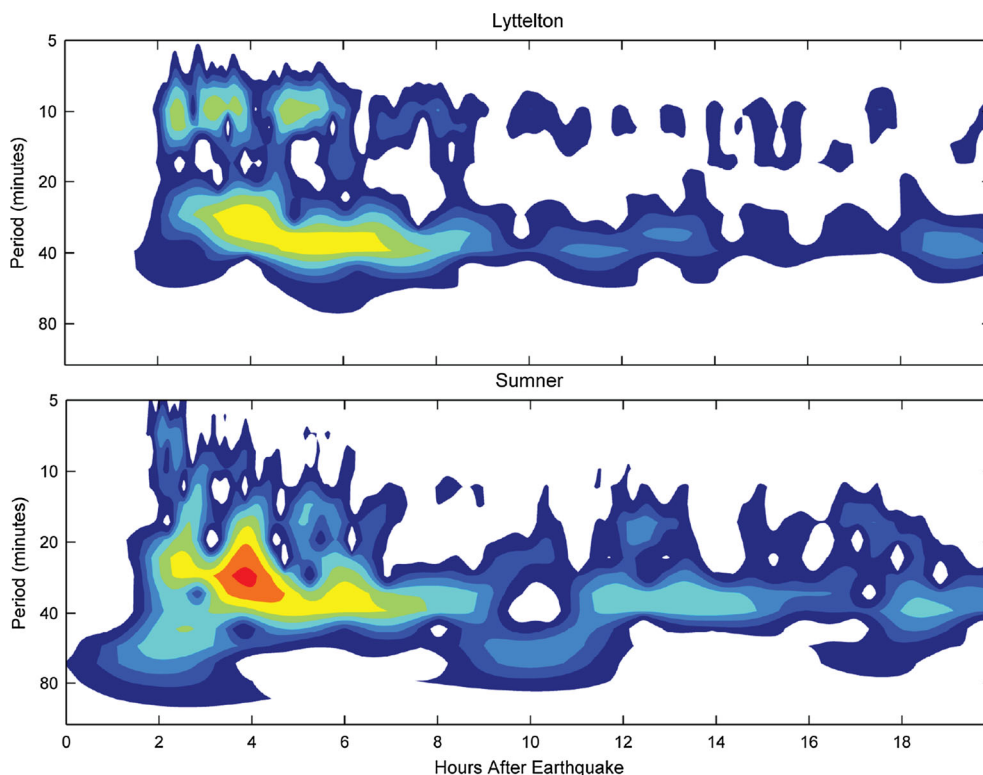


Figure 6
Wavelet spectrogram of the filtered Lyttelton (*top*) and Sumner (*bottom*) tsunami time series

between 2:30 a.m. and 5:00 a.m.. Many of these waves had periods of around 10 min which correspond to the transverse mode of the Lyttelton Harbour seiche (Borrero and Goring 2015). The maximum recorded excursion of the water level due to the tsunami on one cycle (1.2 m trough-to-peak) was also at Sumner. However, this did not count as one ‘wave’ due to the way waves are defined during the zero-crossing analysis. This resulted in the wave cycle occurring around 4 a.m. to be counted as two waves. The first started at 3:20 a.m., rose to +0.31 m then dropped to -0.57 m before returning to zero at 3:53 a.m.. This was followed by the next wave which went up to +0.63 m then down to -0.35 m before coming back to zero at 4:23 a.m.

The spectral content of the filtered water level time series was quantified using wavelet analysis which follows the evolution of the frequency content over the duration of the tsunami. Wavelet analysis is most appropriate tsunami which contain non-stationary power at many different frequencies due to

the interaction between the incoming tsunami waves and the resonant frequencies of the receiving environment. The method applied here follows Borrero and Greer (2013) and uses a Morlet mother wavelet as that shape is most useful for identifying changes in frequency components over time and because its moderate width in both the time and frequency domain allows for reasonable resolution in both dimensions (Torrence and Compo 1998).

The wavelet spectrogram presented in Fig. 6 shows the presence of both the longitudinal (~ 40 min) and transverse (~ 10 min) Lyttelton Harbour seiche and confirms the zero crossing analysis presented above. The peak in tsunami energy can be clearly seen approximately 4 h after the earthquake (around 4:00 a.m.). Notably, this local Kaikōura tsunami did not excite the Pegasus Bay seiche which is the fundamental mode of shelf resonance in the Canterbury Bight with a period of 205 min (Goring and Henry 1998). While there was some energy at this frequency on 14 November 2016,

it was a similar amount to that present the previous day. This seiche has been excited in previous far-field tsunamis (Borrero et al. 2014; Borrero and Goring 2015).

3. Field Observations and Interpretations

3.1. Little Pigeon Bay

Little Pigeon Bay is a small, funnel-shaped bay on the northern side of Banks Peninsula (Fig. 1). As mentioned above, on 14 November 2016, it was reported that the historic cottage on the beach at Little Pigeon Bay had been badly damaged by the tsunami.

Four post-tsunami surveys were carried out at Little Pigeon Bay: 16 November 2016 (two days after the event); 19 November 2016 (after a heavy rain storm on 17 November); 30 November 2016 (16 days after the event); and 15 January 2017 (62 days after the event). The intent was to document the effects of tsunami inundation and also the temporal changes of the inundation signature. The landowners were present during the first visit and were able to indicate places where they had already started the clean-up process and where inundation markers had already been removed.

3.1.1 Evidence of Inundation

On Wednesday 16 November, two inundation lines were visible, as outlined by rafted seaweed and organic debris (Fig. 7). Dead fish, crayfish (*Jasus edwardsii*), kina (*Evenchinus chloroticus*) and paua (*Haliotis iris*) shells were scattered over the grass. Seaweed was caught up in trees, fences and the house foundations. The macrocarpa (*Cupressus macrocarpa*) wind-break showed a clear inundation line of small seaweed floats, twigs and debris caught up in the branches as the water strained through it. The front and sides of the house were covered in tsunami “speckle” (small pieces of seaweed and organic material spattering the walls). On the seaward side of the house it reached the underside of the veranda roof (approximately 5 m above NZVD2016). As the day progressed and the sun warmed the building, the “speckle” fell off the newer weatherboards but remained attached to the cooler sides of the house that were sheltered from the sun.

While there was no obvious tsunami deposit visible, except for sediment in the house, a closer inspection of the surrounding area revealed that a thin veneer of sand had been deposited by the tsunami, but that it was hidden within the grass. This sediment appeared qualitatively similar to that left inside the house.



Figure 7

Inundation indicators (*white dashed lines*): **a** upper and lower inundation lines indicated by organic debris (16 November 2016, photo: William Power). **b** Logs at the bend in the stream were transported upstream by the tsunami. The inundation line can be seen on the far side of the stream (14 November 2016, Photo: Penny Aitkens)

Large cut sections of tree trunks that had been lying on the beach were transported inland by the tsunami. One came to rest after pushing in the door of the shed behind the house (Fig. 8), while others hit the house or were washed out into the bay by the backwash. One large tree trunk was lodged in seafloor sediments partway out into the bay. A power pole was also picked up and deposited 5 m inland from its original position (Fig. 8). The veranda was ripped off the side of the house and deposited on the beach, floating away on the subsequent high tide. It was retrieved and moored to nearby trees by the land-owners. Two logs with diameters of 20 and 40 cm

were also deposited in the streambed up to 120 m inland (Fig. 7).

The owners reported that the back lean-to of the house had previously been inundated by storm surges running up the streambed and sweeping around into this lower section of the property (floor level 2.4 m above NZVD2016). This had occurred at least twice during large storms in 2015, but storm surge inundation had never penetrated into the main part of the house (which is on foundations with a floor level about 0.27 m higher than the concrete slab floor of the lean-to). The owners also reported that the 1960 tsunami had left a sand deposit throughout the house,



Figure 8

Inundation indicators: **a** logs and seaweed deposited by the tsunami (14 November 2016, Photo: Penny Aitkens). **b** Veranda and other tsunami debris floating in the bay after the tsunami (14 November 2016, Photo: Penny Aitkens). **c** Log battering ram (in photo it has already been cut in two for transporting, and had been moved by the time of the first survey). The *lower inundation line* (see also Fig. 9) can be seen below the log (*white line*) (14 November 2016, Photo: Penny Aitkens). **d** Power pole that was moved by tsunami (16 November 2016, photo: William Power)

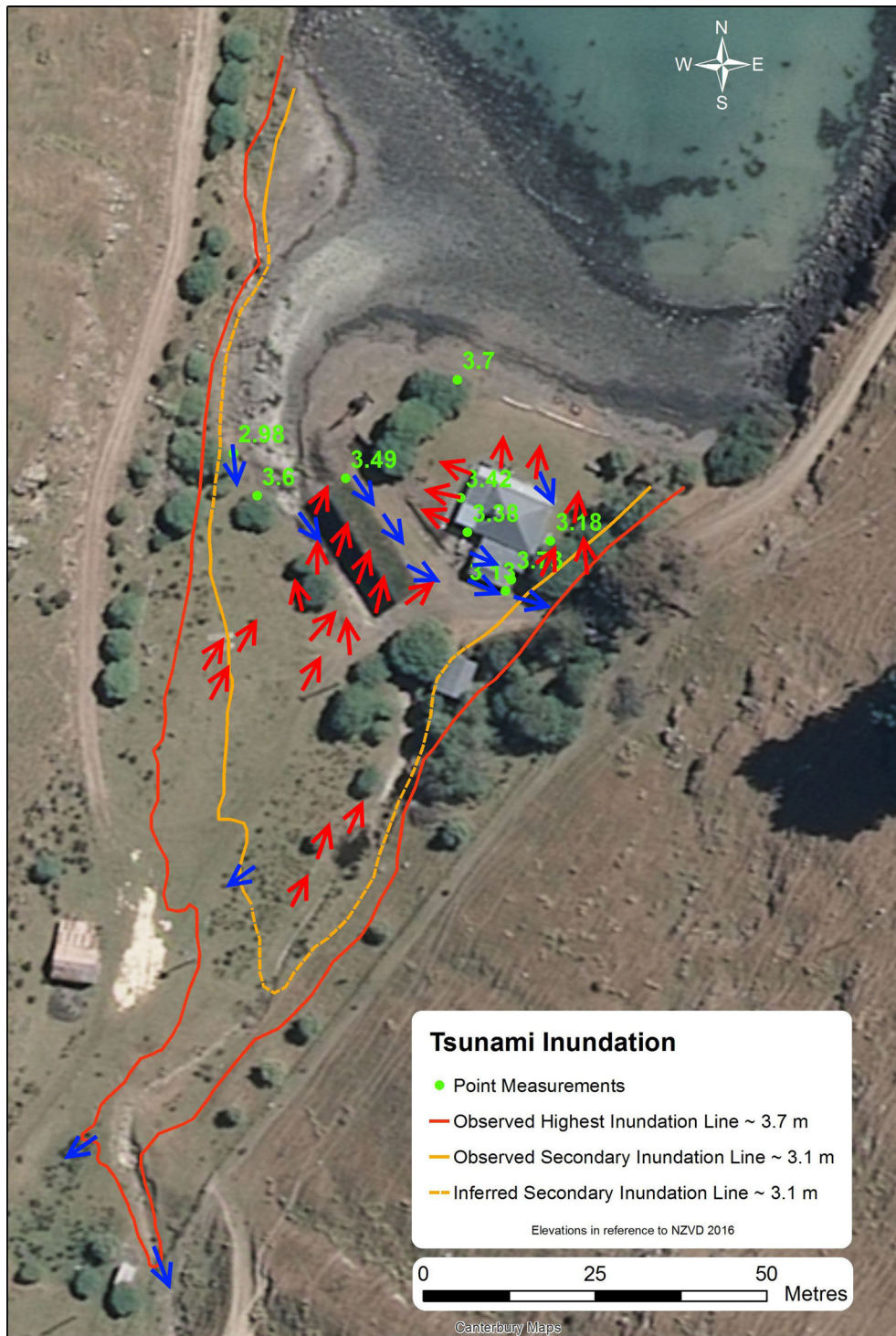


Figure 9

Map of tsunami inundation lines; point measurements of minimum tsunami inundation heights, relative to NZVD2016 and flow indicator directions (*blue* as inferred uprush and *red* inferred backwash). Note that the run-up distance in the streambed is at the fence, where seaweed was found—seawater may have inundated slightly further inland but no debris evidence was apparent as it was strained out in the fence.

Location of map is 172.90°E 43.63°S

but had not caused structural damage (Edward Aitkens, pers. comm., November 2016) so it is unlikely to have weakened the structure. Sand deposits laid down by the 1960 tsunami have also been reported from Purau Bay and Port Levy, to the west of Little Pigeon Bay (Fig. 1) (Goff et al. 2015). Similarly, sand and debris were observed in Okains Bay, Lavericks Bay, Le Bons Bay and Goughs Bay, four east facing bays on Banks Peninsula (Fig. 1), following the 1960 event, although there were no reports of damage to infrastructure (Donnelly et al. 2016; Kain et al. 2016; Goff, unpublished data). In Teddington, Lyttelton Harbour (Fig. 1) there were only reports of flooding, although recent studies have identified sand and discontinuous mud layers at different sites, both being attributed to the event (Goff 2005; Judd et al. 2017). The 1960 tsunami, however, caused structural damage to a bridge in Pigeon Bay (Fig. 1) (E. Perry, pers. comm., November 2016) and electrical equipment at Lyttelton Port (de Lange and Healy 1986).

Figure 9 shows the two inundation lines, in addition to point measurements of minimum inundation heights inferred from seaweed, inundation lines on outside walls of the cottage and other debris markers. The highest run-up distance/maximum limit of inundation is 140 m inland with a run-up height of 3.7 m above NZVD2016. This is approximately 28 cm above current mean sea level at the nearby Sumner sea level gauge (Reeve and Bell 2013). A second inundation line reached about 100 m inland, with a run-up height of 3.1 m above NZVD2016. Both of these inundating waves would have affected the cottage and the lower wave necessarily came after the first that would have removed evidence for any earlier, smaller waves.

3.1.2 Flow Patterns

Imbricated rocks, flattened grass, rafted material, seaweed and other debris caught in fences, trees and house foundations indicated several flow directions. Arrows show these flow directions in Fig. 9; blue arrows denoting inferred uprush and red arrows denoting inferred backwash. Imbricated rocks in the streambed near the macrocarpa wind-break indicate that water travelled up the streambed

at speeds able to align rocks with an 'a' axis up to 15 cm. Farther up the valley, most of the observed tsunami flow directions documented the backwash of the tsunami. However, in the rush-covered flat areas between 60 and 100 m inland to the west of the stream, and also around 120 m inland near the bend in the stream, the occasional sign of rafted material indicated where the tsunami wave reached its maximum extent. The macrocarpa wind-break provided interesting flow information. Based on debris trapped in it, the southern side of the wind-break showed evidence of water running out towards the north which we interpret as backwash. The northern side showed a southeasterly flow direction (blue arrows). We interpret this pattern to be uprush of the incoming wave flowing around from the streambed towards the house. Given the dense nature of the macrocarpa wind-break it is not surprising that the two sides presented evidence of different wave directions because most of the debris that record the flow direction (e.g., seaweed, rags) would be strained out on the upstream side of the flow. Flow directions at the back of the house showed water flowing ESE, wrapping around the building and returning to sea (the narrow corridor between the back of the house and the hill on the eastern side focussed the flow, with water flattening the surrounding grass). Backwash also flowed under the house from the rear and exited out of the north-facing front and western side, leaving debris trapped in the piles. Additionally, tsunami "speckle" on the front veranda reached up to the underside of the roof and was considerably higher than any other inundation marks (up to 5 m above NZVD2016). This suggests that one wave approached the property from a northerly/north-westerly direction splashing up onto the house. The stoving-in of the front door of the cottage suggests that this was a debris-laden wave.

We hypothesise that part of the tsunami went over the beach to hit the cottage front on (from the north) while some of the wave followed the path of the dry streambed up the valley spilling out onto the flat ground beside the stream. A portion of the wave that travelled up the streambed also wrapped around the back of the cottage (from the W) causing damage (see Sect. 3.1.3 for details) and the

backwash of water swept around the eastern side of the house in a narrow corridor between the house and the hillside.

3.1.3 Damage to Cottage

The cottage at Little Pigeon Bay sustained heavy damage during the tsunami. The three primary causes of damage were uplift forces, debris impacts and sediment deposition. Uplift forces completely removed the veranda along the western side of the cottage, and part of the northern veranda (this was never recovered). The western end of the cottage was also lifted approximately 5 cm from its foundations. Debris impacts destroyed veranda posts on the seaward side of the cottage, removed the front door and displaced several of the walls inwards. The maximum wall displacement due to debris impact was approximately 70 cm adjacent to the front door. The tsunami deposited sediment on the floor of every room of the cottage, with finer material plastered on the walls providing a clear indication of internal inundation (and/or splash) levels. Damage on the northern (seaward) side of the cottage can be seen in Fig. 10.

The water marks and damage to the cottage provide useful data to support the inundation height and direction observations obtained from the inshore debris deposits. Figure 11 shows a water mark measured in the bathroom of the house. However, depending on their location, the water marks were also caused by splashing (where the water met a vertical wall) or sloshing (in some of the rooms). The external water marks were measured at 3.42, 3.38, 3.13 and 3.73 m above NZVD2016 (see point measurements in Fig. 9). These inundation height observations are supported by the survey of the upper debris line further inland, approximately 3.7 m above NZVD2016. Based on the observed damage (and local topography) the tsunami appears to have impacted the cottage from the north (seaward side—the shortest path to the cottage) and west (following the streambed onshore). The largest debris impacts were sustained from these two directions. The eastern side of the cottage also sustained debris impact during backwash.



Figure 10

Damage observations from the northern (seaward) side of the cottage, showing the deck removed by the uplift forces (*shaded area*), the veranda poles removed or displaced (*dotted lines*) and the location of debris impact on the wall and door (*arrow*) (14 November 2016, photo: Penny Aitken)



Figure 11

Internal water mark in the bathroom approximately 1.0 m above the floor, along with significant sediment deposition on the floor (photo: James Williams)

The vertical uplift forces were the most destructive hydrodynamic forces exerted on the cottage by the up-rushing tsunami wave. Much of the building was lifted slightly, with the most significant uplift occurring at its western end. Two old fireplaces in the central rooms had chimneys built into the foundations that were not uplifted during the event. In contrast, the internal walls of the cottage were uplifted around the fireplaces, causing significant damage to their hearths. Lateral hydrodynamic forces did not appear to contribute significantly to damage of the external walls of the cottage, and the water depth around the outside was not high enough to affect the windows.

The tsunami deposited sediment and fine debris on the walls and floors of every room. Although the most severe damage was caused by uplift forces and debris impacts, the wetting and sediment deposition ruined most of the furniture within the house. Detailed observations of the damage to the cottage will support the calibration of physical and numerical models of the event, in addition to contributing to research on the development of fragility curves for wooden buildings under tsunami inundation. These

curves will help to quantify the resilience of such buildings, as well as the indicative economic costs of different damage states.

3.1.4 Temporal Changes After the Tsunami

On the first visit, two days after the tsunami, the inundation lines were clearly visible with rafted seaweed and organic debris. Despite a heavy rain storm on 17 November 2016, these inundation lines were still clearly visible during the second visit five days after the event. Some thistles (*Cirsium arvense*) near the beach were beginning to die back—presumably as a result of saltwater inundation. Water flowed in the ephemeral stream after the rain storm and the water in the pond (~ 70 m inland) was notably less brackish on the second visit. The electrical conductivity (EC), a measure of salinity (EC of seawater: $53,000 \mu\text{S cm}^{-1}$, brackish/freshwater limit: $2000 \mu\text{S cm}^{-1}$; e.g., Chagué-Goff et al. 2012), reached $18,310 \mu\text{S cm}^{-1}$ on 16 November 2016, but had been diluted to $1458 \mu\text{S cm}^{-1}$ by 19 November. Two weeks later, on 30 November



Figure 12

Comparative pictures of bare earth in front of the macrocarpa wind-break. **a** Taken on 19 November 2016. **b** Taken on 30 November 2016. The larger rocks and wooden post can be used as reference points as they have not moved between the two photos. The salt crust was not visible directly after the tsunami (**a**) but is clearly visible 16 days after the event (**b**) (photos: Jose Borrero and Emily Lane)

2016, the pond was filled with freshwater (EC $800 \mu\text{S cm}^{-1}$).

The most striking change over the visits to the site was the occurrence of salt crusts on the third visit (16 days after the event). They were observed in front of, and under the macrocarpa wind-break (Fig. 12), on the streambank and walls of the streambed (Fig. 13). These salt crusts had not been observed during the first two visits, and are attributed to evaporation and capillary action due to temperature and/or wind. Similar crusts have been previously reported following large tsunamis (e.g., Chagué-Goff et al. 2012). In Japan, extensive salt crusts were observed, two months after the 2011 Tohoku-oki tsunami, despite being subject to 60 mm of precipitation (Chagué-Goff et al. 2012); or one year later in areas that were inundated by seawater for 3 months (Chagué-Goff et al. 2014). Here, the high

temperatures and north-westerly winds on the day preceding the survey probably contributed to their formation, despite the heavy rainfall on 17 November 2016 (Akaroa rain gauge measured 30.8 mm of rain on that day, Akaroa EWS retrieved from CliFlo 2017). It is also interesting to note that salt crusts were visible in front of and underneath the macrocarpa wind-break, and underneath trees on the stream bank that offered some protection from rainfall. The occurrence of salt crusts on the stream bank is also evidence that the tsunami not only went upstream but also overtopped the bank (Fig. 13a). It is worth noting that although crusts were absent, saltwater signatures were reported nearly three years after inundation by the 2010 Maule tsunami in Teddington, Lyttelton Harbour (Judd et al. 2017).

On 30 November, the inundation lines were still visible but were not as clear as in previous visits, with some organic debris probably washed out and/or dispersed during heavy rainfall and strong winds. Additionally, there was some die-back of the grass, especially between the cottage and the shoreline. Compared to the two previous visits there was far more small debris visible in the grass, including broken shells, fish scales and general tsunami debris. This is probably attributed to better visibility following grass die-back. A thin (~ 0.5 cm) grey sandy deposit was still observable near the secondary inundation line.

By 15 January 2017 (62 days after the tsunami), while the grass was noticeably sparser than observed on previous visits, there was no marked difference between the grass that had and had not been inundated. This was likely due to heavy summer rains (the Akaroa gauge measured 137 mm of rain since the tsunami—mostly in 3 events) and the growth of long golden grass seed heads (*Rytidosperma clavatum*) masking any further grass die-back that might have been observed. Tsunami debris was still visible in the grass, especially around the house. While individual debris piles could still be seen along the inundation line, they were no longer obviously a linear feature demarking the inundation limit, again in part due to the long grass with dried seed heads (*Rytidosperma clavatum*) that had grown up (Fig. 14). The salt crust that had been so apparent on 30 November 2016 was still weakly visible directly under a tree on the streambank but not on



Figure 13

Salt crust on the bank and side of the stream. **a** 30 November 2016 (photo: Catherine Chagué-Goff). **b** 15 January 2017 (photo: Emily Lane). Note that the salt crust was observed in areas partly protected from rainfall by the tree canopy. By mid-January all the salt crust on the side of the stream had washed away, and only a poorly defined crust was still visible under the tree (**b**)

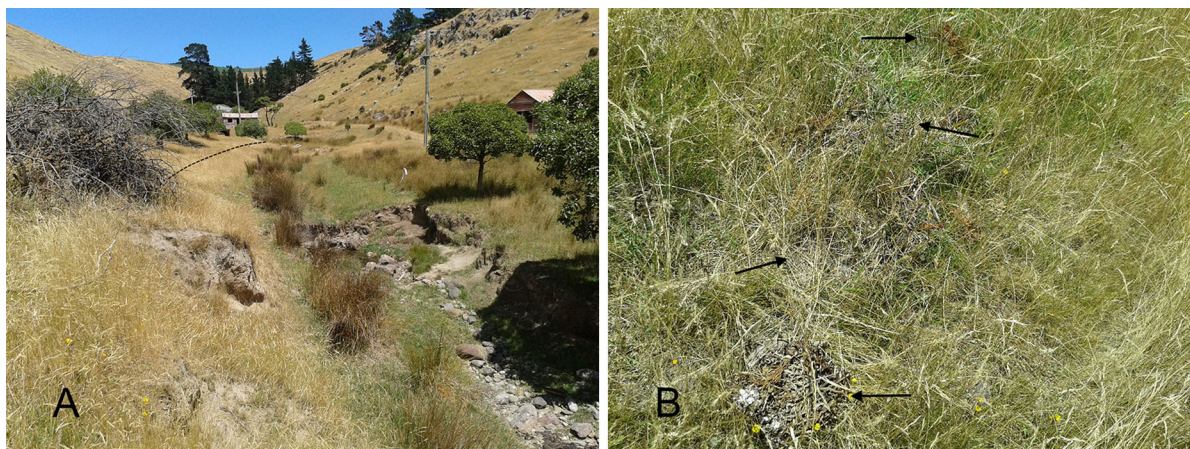


Figure 14

15 January 2017. **a** Any grass die-back that might have occurred was masked by the long golden grass seed heads (*Rytidosperma clavatum*) equally apparent above and below the inundation line (black line). **b** Tsunami debris (black arrows) hidden in the long grass (*Rytidosperma clavatum*) (photos: Emily Lane)

the vertical face (Fig. 13b). Likewise it was visible underneath the macrocarpa wind-break where it was sheltered from the rain but not around the more exposed front section. In both places it was far less striking in colour and extent. While there was still some evidence of tsunami inundation, the extent was harder to determine.

3.2. Pigeon Bay and Other North Facing Bays

Pigeon Bay is a broad embayment adjacent to Little Pigeon Bay. It is shallow at its upper end and is affected by storm surge inundation relatively frequently (Evan Parry, pers. comm., November 2016). The local population was evacuated because of the tsunami risk early on the morning of 14 November 2016 (NZDT). One resident who observed water movements during the early hours of the morning on 14 November 2016 (NZDT) reported that the sea came in and retreated several times (possibly up to 4–5 times) between about 1:30 a.m. and 4:30 a.m. (Evan Parry, pers. comm., November 2016). The first sign was an outrush of water which then surged back in around 2:00–2:30 a.m. at which point it was breaking hard against the sea wall—at about high tide level. About an hour later (3:30–4:00 a.m.) a second uprush was observed which caused a visible surge up the stream and inundation of a low-lying section of

the road (up to 1.7 m above NZVD2016). At daybreak, low-lying parts of the campground (on the eastern side of the bay) were also seen to have been inundated. While the sea was otherwise calm on the day of the tsunami, it occurred during a spring tide event (predicted high tide was 0.85 m above NZVD2016 at the nearby Sumner gauge). Inundation of the road and campground were not seen as particularly unusual, since the shallow upper part of Pigeon Bay amplifies storm surges and so inundation occurs every few years (Evan Parry, pers. comm., November 2016).

On 19 November 2016 several other north-facing bays on Banks Peninsula (Big Bay, Blind Bay (collectively known as Double Bay), Decanter Bay and Menzies Bay) were visited to compare the tsunami inundation with that at Little Pigeon Bay (see Fig. 1). Debris line surveys were carried out at Big Bay and Decanter Bay. However, their remoteness meant that they could not be tied back to a survey datum bench-mark, so elevations are referenced to sea level at the time. The conversion to height above NZVD2016 assumed that the sea level at the time of survey was the same as the nearby Sumner gauge (Fig. 1). Impacts of the tsunami were discussed with landowners/residents at each of the bays visited. Big Bay showed some evidence of inundation just beyond the regular high storm-tide

mark with the possibility of a small surge overtopping the beach berm and penetrating a short distance upstream. The run-up reached approximately 2.6 m above NZVD2016. Blind Bay is a steep, high energy environment and there was no evidence that the tsunami reached any further than the high tide debris line. Likewise, at Decanter Bay and Menzies Bay there was no evidence that the tsunami reached any further than the high tide debris line. At Decanter Bay there was evidence of seawater intrusion up the stream. However, a conversation with the local landowner revealed that this was a common occurrence, and that the tsunami cleaned out seaweed left by the last storm-tide event (David Miller, pers. comm., November 2016). The run-up reached approximately 2.8 m above NZVD2016.

4. Preliminary Modelling

Hydrodynamic modelling of the Kaikōura tsunami was conducted to show a possible mechanism for the tsunami effects recorded at Sumner and Lyttelton and the inundation occurring in Little Pigeon Bay. Preliminary propagation modelling (Fig. 15) using the MOST model (Titov and Gonzalez 1997) shows that while most of the wave energy from the tsunami source region would be projected offshore, a clear wave front can be seen propagating southward into Pegasus Bay, then impacting the north-facing shore of Banks Peninsula. We emphasize that due to the complexities of this earthquake and ongoing debate over the precise tsunami source mechanism, this is not intended as a quantitative representation of the tsunami, but rather as a qualitative assessment of likely propagation patterns.

For the local inundation modelling we used the Saint-Venant (shallow-water wave) solver of the Basilisk model (Popinet 2015). The bathymetry of the bay was obtained using a kayak and a depth sounder; topography was obtained using a mobile laser scanner. Technical difficulties on the survey day meant that we were only able to get the topography for the lower part of the valley. Contours from the inundation line measurements were also included to produce a basic digital elevation model (DEM). The hydrodynamic model was forced at the boundary with the

tide gauge reading from the Sumner gauge starting at 1 a.m. when the gauge crossed 0 m above LVD37 (0.4 m below NZVD2016). This modelling revealed a strong fundamental resonance signal along the bay between the head and the small peninsula on the western edge at a period of about 400 s (Fig. 16). This resonance was particularly noticeable between 2:15 a.m. and 3:00 a.m. In the model output, the two waves that arrived around 2:30 a.m. inundated further than the later waves at 4:00 a.m. and 4:30 a.m. The latter were the largest waves measured at the Sumner gauge. Interestingly these later waves did not excite a strong resonant response. The zero-crossing analysis in Fig. 4 shows waves with periods of around 7 min coming in around 2:00 a.m. while later waves tended to have longer periods. Approximating the expected period of the signal following Rabinovich (2009), and assuming a triangular bay with a linearly sloping bottom (see Table 9.3 in Rabinovich 2009) with a length of 1500 m and a depth at mouth of 16 m, gives a wave period of 396 s. Likewise calculation of the modes based on cross-sections along the thalweg of the bay (Wilson 1972) give a fundamental mode of 403 s. These both correlate strongly with the modelled oscillation period. Figure 17 shows snapshots from the maximum modelled water excursion around 2:30 a.m. and the fundamental mode oscillation. The maximum water level predicted by the model (Fig. 17c) reproduces well the observed inundation. Water draining out the stream can be seen during the water minima (Fig. 17a, d) and an eddy off the small headland can be seen in Fig. 17d.

5. Comparison with Other Areas on the Kaikōura Coast

Significantly more damage from inundation was seen at Little Pigeon Bay on Banks Peninsula than anywhere else along the coast south of Kaikōura. While locations along the Kaikōura coast closer to the earthquake uplift experienced higher run-up heights than Little Pigeon Bay, with 5 m over high tide level reported in Oaro/Goose Bay (Power et al. 2017 submitted, this issue), the tsunami went largely unnoticed because the inundation event was confined to the beach and river flats. The waves did not reach

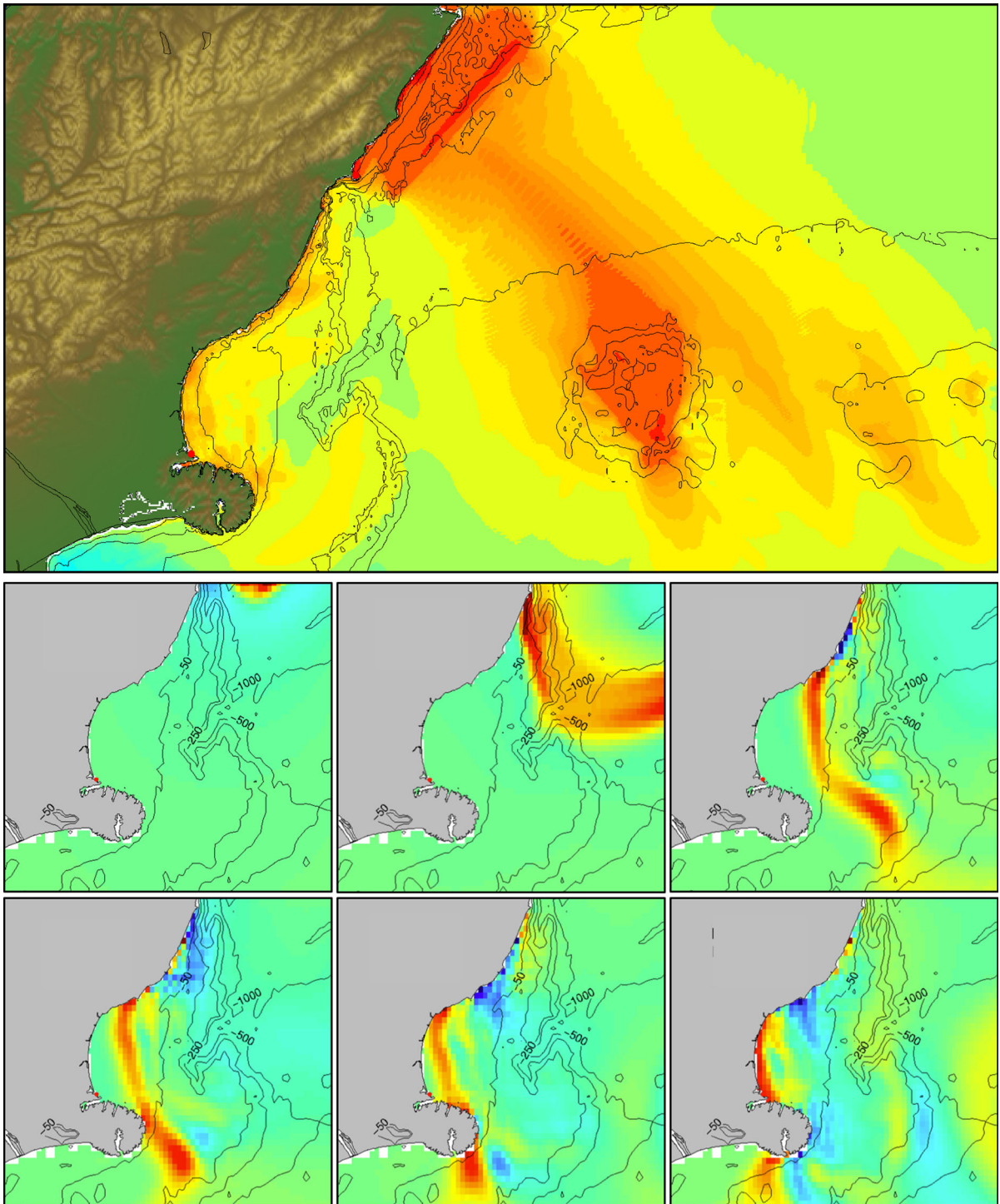


Figure 15

Top Maximum computed tsunami wave heights offshore of the earthquake source region and south to the Banks Peninsula. *Bottom* Snapshots of tsunami wave propagation showing a wave front propagating south towards the north facing coast of the Banks Peninsula

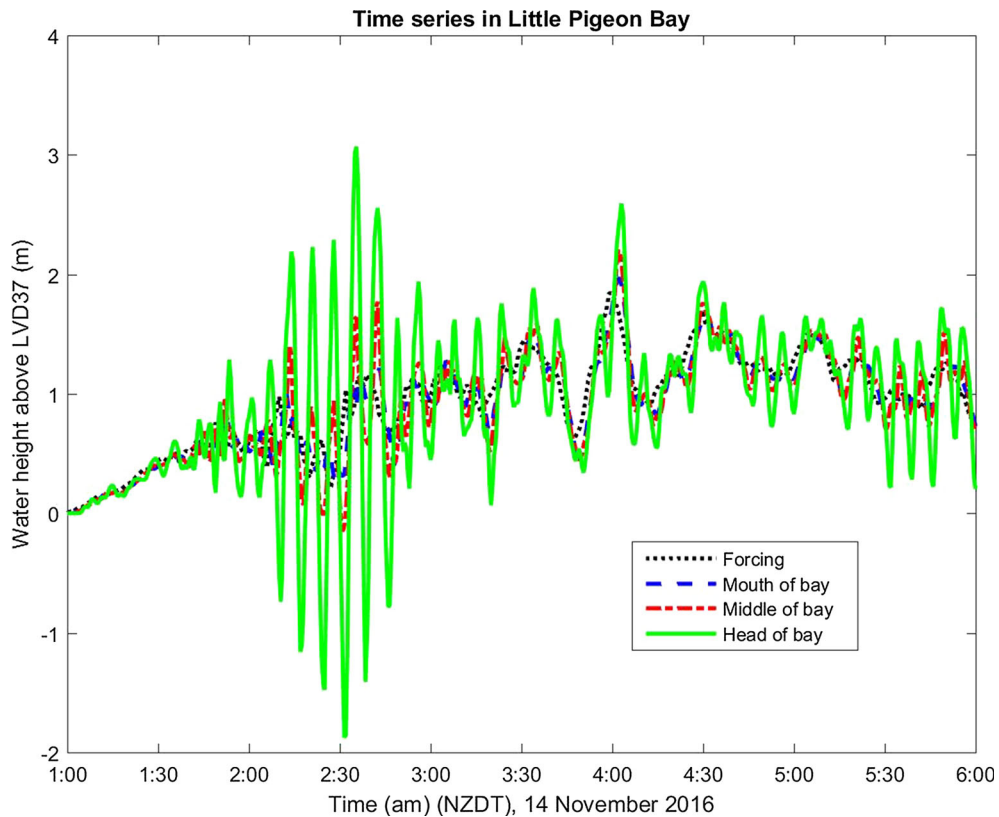


Figure 16

Preliminary modelling of Little Pigeon Bay showing tsunami forcing (Summer tide gauge from 1 a.m. to 6 a.m., 14 November 2016—cf. Fig. 2) and response at the mouth, middle and head of the bay. A strong resonance at the fundamental mode can be seen at the middle and head of the bay

low-lying properties, nor did they cause any damage to infrastructure. This is partly due to the steep beaches in that area. Only a run-up exceeding 5 m would overtop the beach berm in most locations: beyond the limit of this event. In addition, many places in the Kaikōura region underwent significant uplift during the earthquake (Kaikōura itself was uplifted by approximately a metre (Kaiser et al. 2017), increasing the tsunami height needed to overtop the beach berm and cause noticeable inundation. Furthermore, the Kaikōura tide gauge indicates that the largest wave arrived close to low tide.

Run-up in Little Pigeon Bay was at least a metre higher than any of the other north facing bays on Banks Peninsula and it was the only bay on Banks Peninsula where there was significant inland inundation. At least two waves inundated over 100 m inland. There were no eyewitness accounts of the

tsunami's arrival in Little Pigeon Bay. The nearby Sumner sea level gauge (an open ocean gauge approximately 13 km WNW from Little Pigeon Bay, see Sect. 2; Fig. 1) and an eyewitness account of the tsunami in the adjacent Pigeon Bay (see Sect. 3.2) both indicate that the largest wave arrived around 4:00 a.m. NZDT. The second largest wave occurred shortly afterwards at 4:29 a.m. NZDT (high tide was 4:33 a.m. NZDT). However, preliminary modelling of the tsunami in Little Pigeon Bay (Sect. 4) suggests that the tsunami may have excited the fundamental mode of the bay and caused a series of large waves with periods around 7 min between 2:00 a.m. and 3:00 a.m. that may have exceeded the absolute heights of the later waves. Because of the uncertainty in the arrival times of the inundating waves (and hence a possible tidal stage ranging from 0.4 to 0.85 m above NZVD2016) we present a range of run-

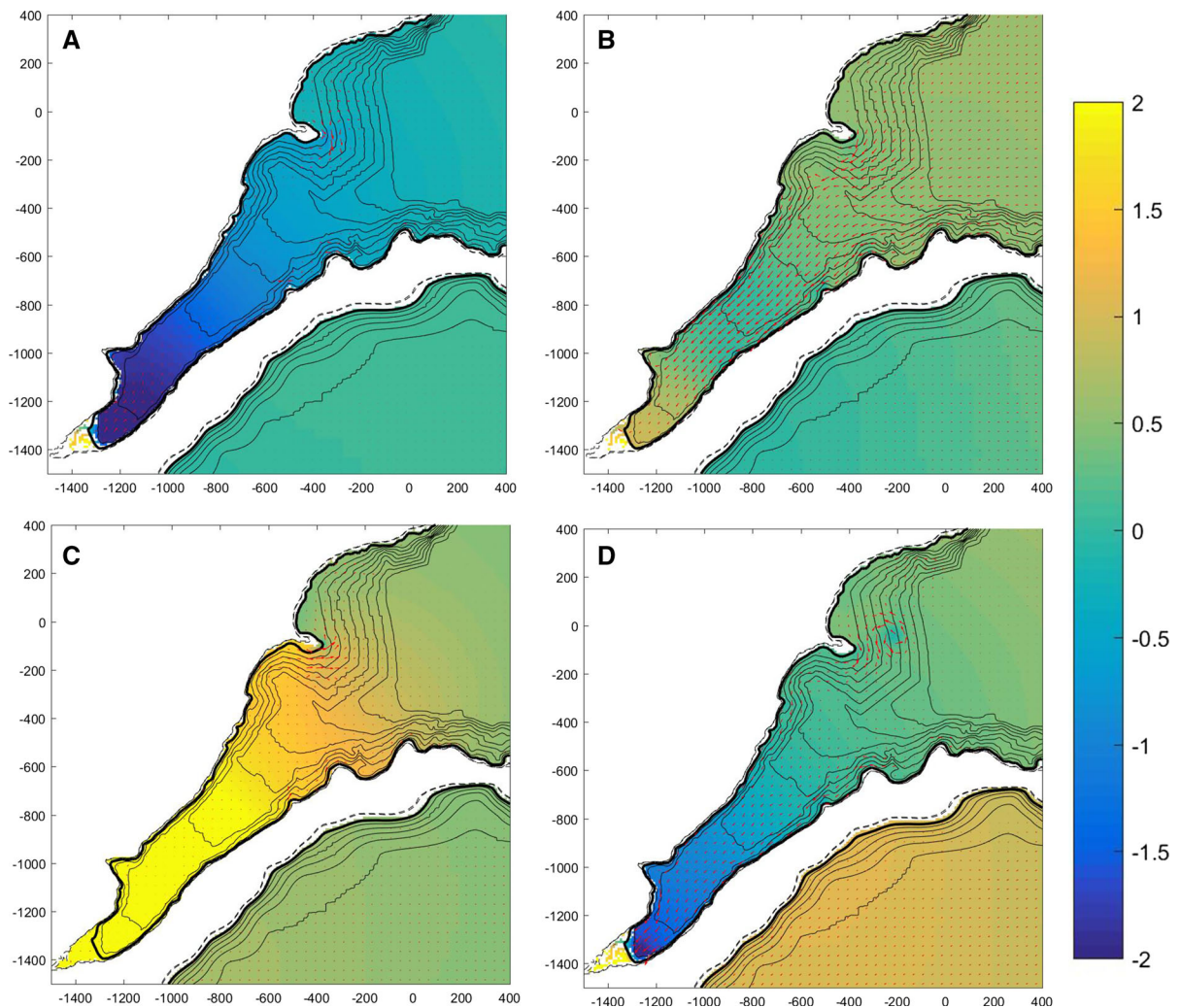


Figure 17

Preliminary modelling of Little Pigeon Bay at bottom of wave at 2:31:30 a.m. (a), inrush at 2:33:30 a.m. (b), maximum water level at 2:35:30 a.m. (c) and next low point at 2:39:05 (d). Contours indicate bathymetry with *bold contour* indicating mean sea level and *dashed contour* indicating maximum inundation extent in Little Pigeon Bay. Note: domain has been rotated so bay entrance is parallel to domain edge

up heights above quiescent water level. Tsunami run-up height due to the largest inundating waves was between 2.9–3.3 m above quiescent water level and 2.2–2.6 m due to the secondary inundating wave (larger if they arrived earlier).

6. Conclusion

The tsunami generated by the November 14 2016 (NZDT) Kaikōura Earthquake was recorded on sea level gauges along the eastern coast of New Zealand.

Beyond Kaikōura, the Sumner gauge recorded the largest response. The most damage caused by the tsunami was observed in Little Pigeon Bay, a small funnel-shaped embayment on the northern side of Banks Peninsula, where the geomorphology and resonance of the bay focussed tsunami energy, increasing inundation extent and run-up heights. A small historical cottage immediately behind the beach berm was severely damaged, with destruction exacerbated by sawn tree trunks on the beach that were transported inland by the tsunami. Four post-tsunami surveys were carried out on 16 November, 19

November, 30 November 2016 and 15 January 2017 to record inundation and run-up heights, and tsunami deposits, as well as temporal changes to this evidence. While only a thin discontinuous sandy deposit was recorded, biological debris was more common. Despite a heavy rain storm three days after the event, a salt crust was also observed in some places two weeks after the tsunami. Sixty days after the event, salt crusts and other debris were less visible as vegetation recovered. Preliminary modelling of Little Pigeon Bay with high resolution bathymetry identified a fundamental resonance with a period around 7 min that could have been excited by the tsunami waves, potentially explaining the anomalously high run-up recorded. We also note field observations of tsunami inundation in neighbouring bays on Banks Peninsula.

Acknowledgements

We would like to thank all the landowners who allowed us access to their land and shared their knowledge of the area: Edward and Penny Aitkens, owners of Little Pigeon Bay; Stuart Stanley, the owner of Double Bay; David Miller, the owner of Decanter Bay and Harold Menzies, the owner of Menzies Bay. Thanks also to Evan Parry for his observations and local knowledge. Thanks to Julian Sykes and Alison Kohout (NIWA) for collecting the Little Pigeon Bay bathymetry and to Dougal Greer (eCoast) for assistance with the wavelet spectrogram plots. This research was supported by NIWA Taihoro Nukurangi, Natural Hazards Research Platform and GNS Science as part of government core funding. Further thanks to David Huntley, Geological Survey of Canada and an anonymous reviewer who critically reviewed this manuscript.

REFERENCES

- Borrero, J. C., & Goring, D. G. (2015). South American Tsunamis in Lyttelton Harbor, New Zealand. *Pure and Applied Geophysics*. doi:10.1007/s00024-014-1026-1.
- Borrero, J. C., Goring, D. G., Greer, S. D., & Power, W. L. (2014). Tsunami hazards in New Zealand Ports. *Pure and Applied Geophysics*. doi:10.1007/s00024-014-0987-4.
- Borrero, J., & Greer, S. D. (2013). Comparison of the 2010 Chile and 2010 Japan tsunamis in the Far-field. *Pure and Applied Geophysics*, 170, 1249–1274. doi:10.1007/s00024-012-0559-4.
- Chagué-Goff, C., Niedzielski, P., Wong, H. K. Y., Szczuciński, W., Sugawara, D., & Goff, J. (2012). Environmental impact assessment of the 2011 Tohoku-oki tsunami on the Sendai Plain. *Sedimentary Geology*, 282, 175–187.
- Chagué-Goff, C., Wong, H. K., Sugawara, D., Goff, J., Nishimura, Y., Beer, J., Szczuciński, W., & Goto, K. (2014). Impact of tsunami inundation on soil salinisation—up to one year after the 2011 Tohoku-oki tsunami. In Y. Kontar, V. Santiago-Fandiño, & T. Takahashi (Eds.), *Tsunami events and lessons learned: environmental and societal significance. Advances in natural and technological hazard research* (Vol. 35, pp. 193–214). Dordrecht: Springer.
- CliFlo (2017). CliFlo: NIWA's National Climate Database on the Web. <http://cliflo.niwa.co.nz/>. Retrieved 31 January 2017.
- de Lange, W., & Healy, T. (1986). New Zealand tsunamis 1840–1982. *New Zealand Journal of Geology and Geophysics*, 29, 115–134.
- Donnelly, J., Goff, J., and Chagué-Goff, C. (2016). A record of local storms and trans-Pacific tsunamis, eastern Banks Peninsula, New Zealand. *The Holocene*. doi: 10.1177/0959683616670222.
- GeoNet (2016a). New Zealand Earthquake Report, Magnitude 7.8, Mon, Nov 14 2016, 12:02:56 am (NZDT), in GeoNet, ed., Quakes Info, Vol. 2016. <http://www.geonet.org.nz/quakes/2016p858000>. GNS Science. Accessed Dec 2016.
- GeoNet (2016a) Tsunami gauges. <http://www.geonet.org.nz/tsunami/gauges/index.html>. Accessed Nov 2016.
- Goff, J. (2005) Preliminary core study—Upper Lyttelton Harbour. NIWA Client Report CHC2005-151.
- Goff, J., McClintock, J., & Kain, C. (2015). Purau Bay to Pigeon Bay: Searching for tsunamis on the seaward side of Lyttelton Harbour. Environment Canterbury report 15/150. ISBN 978-0-947507-08-4 Web, ISBN 978-0-947507-07-7 Print.
- Goring, D. G. (2008). Extracting long waves from tide-gauge records. *ASCE Journal of Waterway, Port, Coastal, and Ocean Engineering*, 134(5), 306–312.
- Goring, D., & Henry, R. (1998). Short period (1–4 h), sea level fluctuations on the Canterbury coast, New Zealand. *New Zealand Journal of Marine and Freshwater Research*, 32, 119–134.
- Holthuijsen, L. H. (2007). *Waves in Oceanic and Coastal Waters*. Cambridge: Cambridge University Press.
- Judd, K., Chagué-Goff, C., Goff, J., Gadd, P., Zawadzki, A., & Fierro, D. (2017). Multi-proxy evidence for small historical tsunamis leaving little or no sedimentary record. *Marine Geology*, 385, 203–215.
- Kain, C., Wassmer, P., Goff, J., Chagué-Goff, C., Gomez, C., Hart, D., et al. (2016). Determining flow patterns and emplacement dynamics from tsunami deposits with no visible sedimentary structure. *Earth Surface Processes and Landforms*. doi:10.1002/esp.4020.
- Kaiser, A., Balfour, N., Fry, B., Holden, C., Litchfield, N., Gerstenberger, M., D'Anastasio, E., Horspool, N., McVerry, G., Ristau, J., Bannister, S., Christophersen, A., Clark, K., Power, W., Rhoades, D., Massey, C., Hamling, I., Wallace, L., Mountjoy, J., Kaneko, Y., Benites, R., Van Houtte, C., Dellow, S., Wotherspoon, L., Elwood, K., & Gledhill, K. (2017). The Kaikōura (New Zealand) earthquake: Preliminary seismological report. *Seismological Research Letters*. doi:10.1785/0220170018.

- LINZ (2016) Sea level data downloads. <http://www.linz.govt.nz/sea/tides/sea-level-data/sea-level-data-downloads> Accessed Dec 2016.
- NIWA (2016) Sea levels. URL: <https://www.niwa.co.nz/our-services/online-services/sea-levels>. Accessed Dec 2016.
- Popinet, S. (2015). A quadtree-adaptive multigrid solver for the Serre-Green-Naghdi equations. *Journal of Computational Physics*, 302, 336–358.
- Power, W. L., Clark, K., King D. N., Borrero, J., Howarth, J., Lane, E. M., Goring, D., Goff, J., Chagué-Goff, C., Williams, J., Reid, C., Whittaker, C., Mueller, C., Williams, S., Hughes, M., Hoyle, J., Bind, J., Strong, D., Litchfield, N., & Benson, A. (2017). Tsunami run-up and tide-gauge observations from the 14 November 2016 M7.8 Kaikōura earthquake, New Zealand. *Pure and Applied Geophysics* (**submitted to this journal**).
- Rabinovich, A. B. (2009). Seiches and harbour oscillations. In Y. C. Kim (Ed.), *Handbook of coastal and ocean engineering* (pp. 193–236). Singapore: World Scientific Publishing Co.
- Reeve, G., and Bell, R. G. (2013). Sumner Head sea level report: 2011–2012. Client report prepared for environment Canterbury.
- Titov, V. V., & González, F. I. (1997). Implementation and testing of the method of splitting tsunami (MOST) model (No. ERL PMEL-112).
- Torrence, C., & Compo, G. (1998). A practical guide to wavelet analysis. *Bulletin of the American Meteorological Society*, 79, 61–78.
- USGS (2016) M 7.8–54 km NNE of Amberley, New Zealand Preliminary finite fault results for the Nov 13, 2016 Mw 7.9–42.7570, 173.0770 Earthquake (Version 1). <http://earthquake.usgs.gov/earthquakes/eventpage/us1000778i#finite-fault> Accessed Dec 2016.
- Walters, R., Barnes, P., Lewis, K., Goff, J. R., & Fleming, J. (2006). Locally generated tsunami along the Kaikoura coastal margin: Part 2. Submarine landslides. *New Zealand Journal of Marine and Freshwater Research* 40(1), 17–28.
- Wilson, B. (1972). Seiches. *Advances in Hydroscience*, 8, 1–94.

(Received February 14, 2017, revised March 9, 2017, accepted March 11, 2017, Published online April 4, 2017)